Proceedings of the Institute of Acoustics

SUPPRESSION OF PLATE VIBRATIONS USING A MODIFIED INERTIAL ACTUATOR

L Benassi Institute of Sound and Vibration Research, Southampton, SO17 1BJ, England
SJ Elliott Institute of Sound and Vibration Research, Southampton, SO17 1BJ, England

1 INTRODUCTION

Vibration control of flexible structures is an important issue in many engineering applications, especially for the precise operation performances in aerospace systems, satellites, flexible manipulators, etc. Balancing the stringent performance objectives of modern structures such as superior strength and minimal weight introduces a dynamic component that needs to be considered. Two types of control methods are generally used to solve this problem: passive control and active control. Passive vibration control and the use of tuned systems can be effective on single frequency vibrations[1]. This work considers the possibility of broadband control of a distributed system, such as a flexible panel, using local vibration controllers.

In this paper, the total power generated by the forces exerting on the structure is used as a function to be minimised[2]. This approach has also been used in active sound control[3]. If we assume the system to be linear such that the velocity fields produced by the forces can be superimposed, then the total power has a known minimum value that is associated with an optimal solution[3]. The ratio of the optimal secondary force and the resultant velocity at the secondary force location is termed the equivalent impedance of the active control system. Unfortunately, a drawback of the optimal equivalent impedance is that it is non-causal[4] and so cannot be implemented for broadband random excitations.

A lot of work has been carried out in order to synthesize load impedances which achieve desired performances, and in this study optimal impedances and sub-optimal impedances generated by passive and active devices will be compared. The goal is to use these devices in order to achieve global control, acting on a local basis. In particular, the use of inertial actuators in active vibration suppression systems is investigated. Inertial actuators do not need to react off a base structure, so that they can be used as modules that can be directly installed on a vibrating structure. It has previously been shown, however, that in order to implement stable skyhook damping with an inertial actuator, the natural frequency of the actuator must be below the first resonance frequency of the structure under control and the actuator resonance should be well damped[5]. A novel device for active vibration control, based on an inertial actuator with displacement sensor and local PID controller and an outer velocity feedback control loop, is used to control the vibrating flexible plate. The impedance presented to the plate by this actuator is compared with the equivalent impedance of the optimal active control system. A frequency-domain formulation is used to analyse the stability and performance of an active vibration suppression system using this modified inertial actuator.

A vibrating flexible finite plate will be considered in Section 2 and its equivalent impedance for optimal global control will be described. In Section 3, the use of sub-optimal impedances will be considered, followed in Section 4 by the application of the new device to a vibrating plate. In Section 5, the vibration suppression of a flexible plate is investigated experimentally, using the modified inertial actuator. In Section 6, the effect of installing the modified inertial actuator at different locations on the flexible plate is analysed. Finally in Section 7 some overall conclusions are drawn.

2 OPTIMISED IMPEDANCE FOR GLOBAL CONTROL OF VIBRATING FINITE PLATES

In order to apply the optimal solution to a finite plate, we examine a single point secondary force, f_s, acting at a point $P_1 = (x_1, y_1)$, separated by a distance r from a point primary force, f_p, acting at a point $P_0 = (x_0, y_0)$, both forces being applied along the z-axis on a finite plate. This configuration

is depicted in Fig. 1(left). In the simulations it is assumed that the 700 x 500 x 1.85 mm plate is clamped on two opposite ends and free to move on the other two. Y_{00} is the driving point mobility at P_0, defined as $Y_{00} = \frac{\dot{z}_0(\omega)}{f_0(\omega)}$, where $\dot{z}_0(\omega)$ is the velocity in the *z* direction evaluated at P_0, and $f_0(\omega)$ is the excitation force at P_0. Y_{10} is the transfer mobility when the point of excitation is P_0 and the measurement occurs at P_1, and Y_{11} is the driving point mobility at P_1. The driving point and transfer mobilities for this system, relating the vertical velocity and the force excitation at the locations P_0 and P_1, can be derived using a modal superposition approach[7,8].

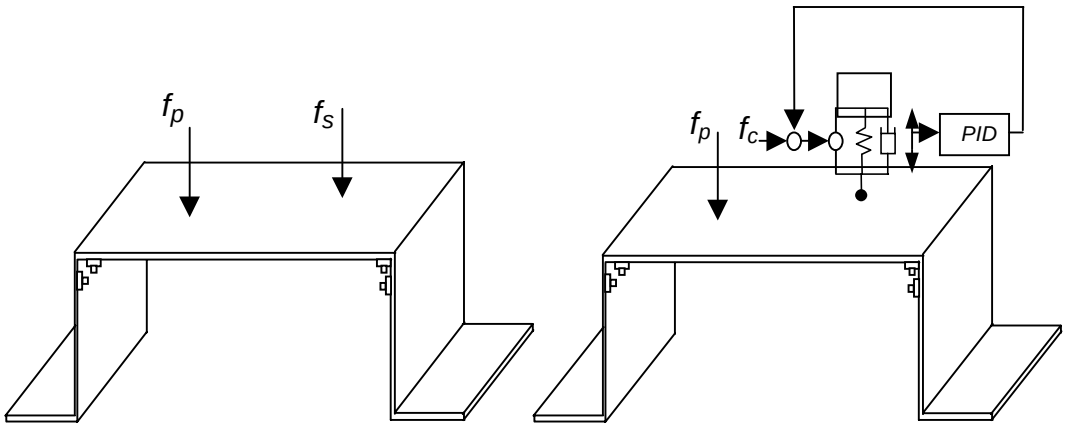

Figure 1. Left: a point primary force and a point secondary force applied to a finite 700 x 500 x 1.85 mm plate clamped on two opposite edges and free on the other two edges. Right: a point primary force and a point secondary force, obtained through the modified inertial actuator, applied to a 700 x 500 x 1.85 mm plate. The plate is clamped on two opposite edges and free on the other two edges.

It is possible to define a cost function that will be used as the reference for all the remaining computations. The chosen cost function is the total power supplied to the plate, which is given by the sum of the power Π_p due to the primary force acting in P_0 and the power Π_s due to the secondary force acting in P_1. It can be expressed as

$$\Pi = \Pi_p + \Pi_s \tag{1}$$

and rewritten considering that the total power is also one half of the real part of the forces times the complex transverse velocity of the plate at the position of the application of the forces. This total power can also be written as[9]

$$\Pi = \frac{1}{2}\mathrm{Re}\left\{f_p^* v_p + f_s^* v_s\right\} = A\left|f_s\right|^2 + f_s^* b + b^* f_s + c\,, \tag{2}$$

which is a quadratic form where the parameters of the last term of equation (2) are

$$A = \frac{1}{2}\mathrm{Re}(Y_{11})\ ,\ b = \frac{1}{2}\mathrm{Re}(Y_{10})\,f_p\,,\ c = \frac{1}{2}\left|f_p\right|^2\mathrm{Re}(Y_{00})\,. \tag{3}$$

In particular, the power of the primary force only, which provides the power of the system without any sort of treatment, is given by setting the secondary force in equation (2) to zero. This leads to

$$\Pi_p = c \ . \tag{4}$$

Equation (2) has a well-defined minimum value[9]

$$\Pi_{opt} = c - \frac{|b|^2}{A} \ , \tag{5}$$

which is associated with an optimal secondary force f_{so} given by

$$f_{so} = -\frac{b}{A} = -\frac{\mathrm{Re}(Y_{10})}{\mathrm{Re}(Y_{11})} f_p \ . \tag{6}$$

The solid line in Fig. 2(left) shows the power supplied to the finite plate due to the primary force only, applied at an arbitrary location P_0 = (0.32 m, 0.27 m), and the faint line shows the total power due to the combination of the primary and optimal secondary force, applied at a distance *r* = 2 cm, at a location P_1 = (0.3059 m, 0.2841 m), from the primary location. The reduction is substantial, with some of the modes being almost cancelled, while others are greatly reduced. This is due to the particular location that was chosen for the secondary force. At that location, the secondary force can couple into most modes, but this location is either on or close to the nodal lines of those modes that are not completely flattened out. The impedance that the secondary force has to present to the system in order to minimise the total power is obtained by computing the optimal secondary force, f_{so}, per unit velocity at the secondary location, v_{bo}. The velocity of the base v_{bo} at P_1 when the optimal solution is implemented is given by

$$v_{bo} = Y_{10} f_p + Y_{11} f_{so} \ . \tag{7}$$

Substituting equation (6) into equation (7), the equation becomes

$$v_{bo} = Y_{10} f_p - Y_{11} \left(\frac{\mathrm{Re}(Y_{10})}{\mathrm{Re}(Y_{11})} \right) f_p \ , \tag{8}$$

which represents the velocity as a function of the primary force. Combining equations (6) and (8), the impedance when the optimal secondary force is implemented can be obtained. It is given by

$$Z_{opt} = \frac{f_{so}}{v_{bo}} = \frac{\mathrm{Re}(Y_{10})}{\mathrm{Re}(Y_{10})Y_{11} - \mathrm{Re}(Y_{11})Y_{10}} \ . \tag{9}$$

This equivalent impedance, which is entirely reactive, is shown in Fig. 2(right), where sharp transactions between the stiffness dominated regions and the mass dominated regions occur. Between 0 and about 45 Hz, below the first natural frequency, the impedance is stiffness dominated, as it is between about 60 Hz and 120 Hz, and between 155 Hz and 175 Hz. In the remaining intervals within the 0~200 Hz window, the impedance is mass dominated.
The primary drawback of the optimal equivalent impedance shown in Fig. 2(right) is that it is non-causal[4] and so cannot be implemented for broadband random excitations. Therefore, other solutions must be investigated even though their performance will be worse than that one provided by the optimal solution.

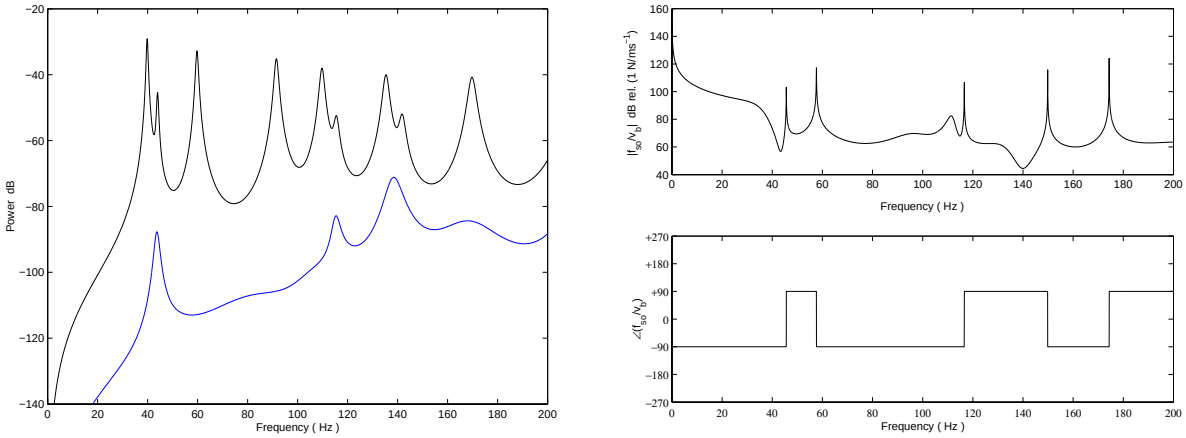

Figure 2. Left: total power transmitted to the finite plate due to the primary force only (solid) and due to the primary and secondary forces when the optimal feedforward solution is applied and the distance between primary and secondary force is 2 cm (faint). Right: equivalent impedance due to the optimal secondary force. The distance between primary and secondary force is 2 cm and the plate is finite. It can be noted that the real part of the impedance is zero.

3 OPTIMISING THE SPRING/DAMPER APPROXIMATION TO THE EQUIVALENT IMPEDANCE

In this section, the combination of an optimum stiffness and a damper will be analysed. Firstly, the two solutions are investigated independently, then they will be considered together, acting in parallel on the finite plate. The relative distance, *r*, between primary and secondary forces is assumed to be 2 cm for these simulations.

Fig. 3(left) shows the ratio of the frequency-averaged power *P* between the power of the uncontrolled and the controlled plate, as a function of stiffness. The function descends monotonically until it flattens off at about $k_a = 9 \cdot 10^6$ N/m, which indicates the minimum value of stiffness that provides the greatest attenuation in power (about 14 dB). At low values of the stiffness, the ratio of the frequency averaged power is very steep. Fig. 3(right) shows the total power when the stiffness is chosen to be $k_a = 9 \cdot 10^6$ N/m (dashed line), compared to the optimal solution (faint line) and the uncontrolled case (solid line). It can be noted that high attenuations can be achieved at low frequency due to the similarity between optimal solution and passive equivalent approximation. Although $k_a = 9 \cdot 10^6$ N/m seems to be a good choice at low frequency, at higher frequency its effect is merely to pin the structure at the secondary location and therefore a redistribution of the resonances is experienced.

Fig. 4(left) shows the ratio of the frequency averaged power as a function of damping c_a introduced at P_1. The minimum of the function at about c_a = 4,000 N/ms^{-1} is –14.5 dB, and it indicates the value of damping that provides the greater attenuation in terms of power. At low gains, the frequency averaged power is very steep then, after reaching a minimum value, it settles towards the constant value –14 dB, which indicates that the system is pinned and it does not benefit from higher damping values. Fig. 4(right) shows the total power when c_a = 4,000 N/m (dashed line), compared to the optimal solution (faint line) and the uncontrolled case (solid line). Compared to Fig. 3(right), lower attenuations are experienced below the first plate resonance and higher attenuations can be achieved at high frequency.

We now assume that the secondary force is generated by a spring and a damper, whose values are chosen by a joint optimisation. Fig. 5(left) shows the contour plot of the ratio of the frequency-averaged power as a function of damping and stiffness. The ratio is maximum at the origin, then it descends. The minimum of the function (about –14.62 dB) occurs when the damping value c_a =

4,000 N/ms^{-1} , which coincides with the minimum of the curve in Fig. 3(left), and the stiffness value $k_a = 5.5 \cdot 10^5$ N/m. Fig. 5(right) shows the total power when the chosen spring-damper system is applied (dashed line). Compared to Fig. 4(right), the system clearly benefits at low frequency from the stiffness, and above the first plate resonance, it benefits from the energy that has been taken away by the damper. Compared to Fig. 3(right) and Fig. 4(right), this case provides a better performance. Unfortunately, in many practical applications a rigid ground is not available and therefore these solutions cannot be implemented.

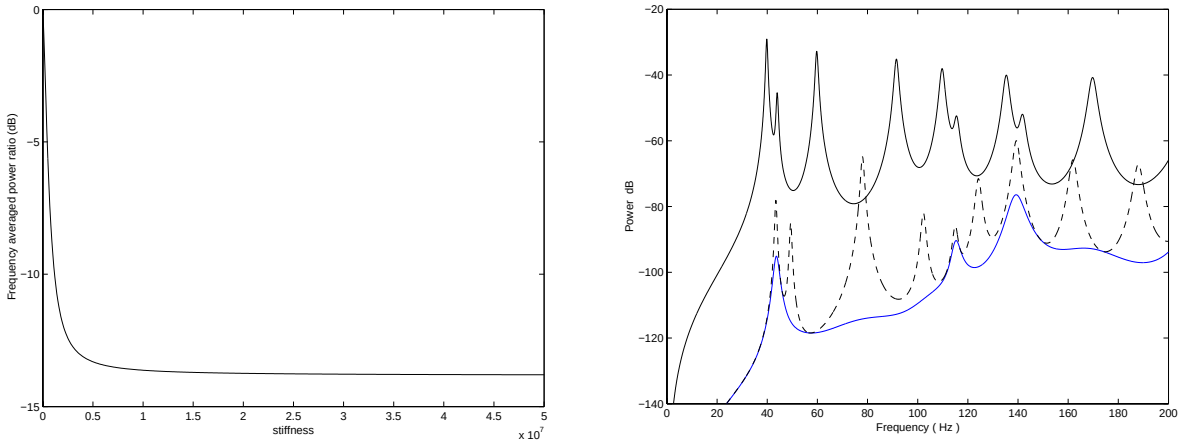

Figure 3. Left: ratio of the frequency averaged power between power of the uncontrolled and controlled plate, as a function of the stiffness value k_a. Right: total power transmitted to the finite plate due to the primary force only (solid), the primary and secondary forces when the optimal feedforward solution (faint), and the primary and secondary forces when the ideal displacement feedback is implemented and the stiffness is $k_a = 9 \cdot 10^6$ N/m (dashed). The distance between primary and secondary force is 2 cm.

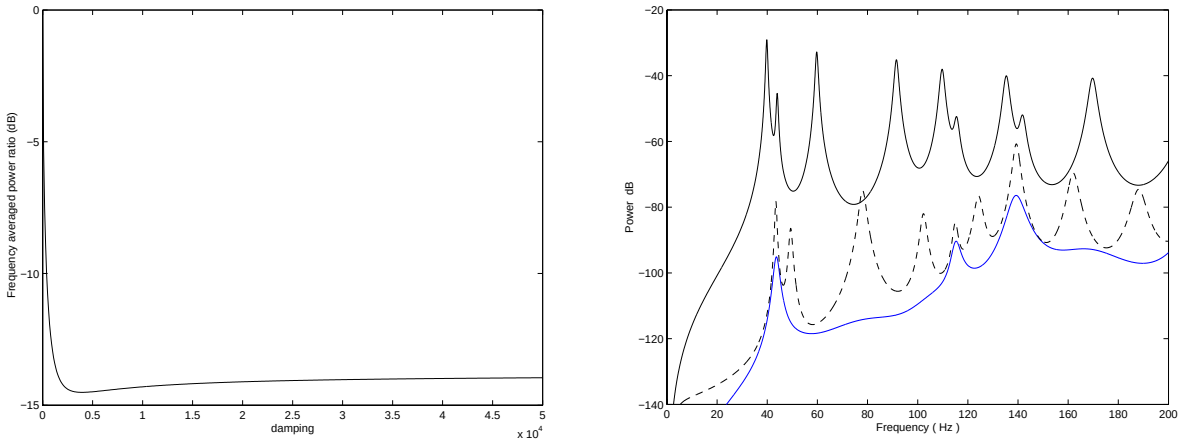

Figure 4. Left: ratio of the frequency averaged power between power of the uncontrolled and controlled plate, as a function of the damping value c_a. Right: total power transmitted to the finite plate due to the primary force only (solid), the primary and secondary forces when the optimal feedforward solution is applied (faint), and the primary and secondary forces when the ideal velocity feedback is applied and the damping value c_a = 4,000 N/ms^{-1} (dashed). The distance between primary and secondary force is 2 cm.

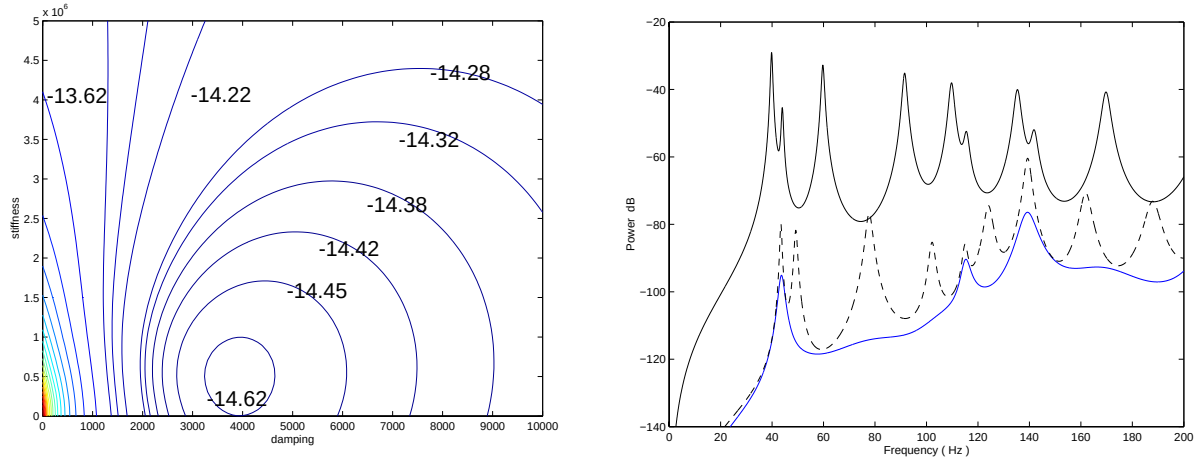

Figure 5. Left: labelled contour plot of the ratio of the frequency averaged power between power of the uncontrolled and controlled plate, as a function of the damping value c_a and the stiffness value k_a . The minimum of the function at –14.62 dB occurs when c_a = 4,000 N/ms^{-1} and k_a = $5.5 \cdot 10^5$ N/m. The distance between primary and secondary forces is 2 cm. Right: total power transmitted to the finite plate due to the primary force only (solid), the primary and secondary forces when the optimal feedforward solution is applied (faint), and the primary and secondary forces when the ideal displacement and velocity feedback is applied, where the stiffness value k_a = $5.5 \cdot 10^5$ N/m and the damping value c_a = 4,000 N/ms^{-1} (dashed). The distance between primary and secondary force is 2 cm.

4 INERTIAL ACTUATOR WITH LOCAL DISPLACEMENT FEEDBACK AND PLATE VELOCITY FEEDBACK ON THE FLEXIBLE PLATE

An inertial actuator has a mass, a “proof-mass”, supported on a spring and driven by an external force. The force in small actuators is normally generated by an electromagnetic circuit. The suspended mass can either be the magnets with supporting structure or in some cases the coil structure. The transduction mechanism which would supply the force to the system is not modelled in detail because its internal dynamics are typically well beyond the bandwidth of the structural response. Fig. 1(right) illustrates the case where a modified inertial actuator[9], based on an inertial actuator with local displacement feedback is installed on the plate[10,11]. The measured displacement of the proof-mass relative to the inertial actuator’s base is fed to a PID controller, which modifies the frequency response of the actuator. If it is necessary to reduce the resonance frequency of the actuator because it is greater or equal to the first structural mode of the system that needs to be isolated, this can be done with a negative position feedback gain. If this action induces unwanted deflections because of the low stiffness of the closed-loop system, then a self-levelling mechanism can be employed, which is based on a integral displacement feedback. By doing so, however, the overall system gets closer to instability and additional damping is needed. Another reason why damping may be necessary is if an outer velocity feedback is to be implemented. It was shown by Elliott *et al.* [5] that this kind of system is conditionally stable and the vicinity to the (-1,0) point in the Nyquist plot depends on how well damped the inertial actuator is. For these reasons the implementation of a local rate feedback control turns out to be very effective in increasing the damping of the actuator. A modified actuator resonance frequency at about 8 Hz was considered sufficient in this case since the first plate resonance is at about 35 Hz. The values within the PID controller that were used in the simulations are: proportional gain g_P = -1000, integral gain g_I = 10,000, and differential gain g_V = 18. The secondary force f_s is equal to the transmitted force f_t

exerted by the device and its equation, as a function of the command signal, f_c, and the plate velocity at P_1, v_b, is given by[9]

$$f_s = f_t = \frac{-\omega^2 m_a}{-\omega^2 m_a + j\omega c_a + k_a + g_P + \frac{g_I}{j\omega} + j\omega g_V} f_c - \frac{\left(j\omega m_a k_a - \omega^2 m_a c_a\right)\cdot\left(g_P + \frac{g_I}{j\omega} + j\omega(g_V + Z_a)\right)}{\left(-\omega^2 m_a + j\omega c_a + k_a + g_P + \frac{g_I}{j\omega} + j\omega g_V\right) j\omega Z_a} v_b \quad , \tag{10}$$

where $Z_a = c_a + \frac{k_a}{j\omega}$. The command force, f_c, will be used to implement the outer velocity feedback control loop. Equation (10) can be grouped as

$$f_t = T_a^{'} f_c - Z_a^{'} v_b \ , \tag{11}$$

where $T_a^{'}$ and $Z_a^{'}$ are the blocked response and mechanical impedance of the actuator, as modified by the local displacement feedback. The base velocity at P_1 is given by

$$v_b = Y_{10} f_p + Y_{11} f_t \ . \tag{12}$$

Substituting equation (11) into equation (12) the base velocity is computed as a function of the primary force f_p and the control command f_c

$$v_b = \frac{Y_{10}}{1 + Y_{11} Z_a^{'}} f_p + \frac{Y_{11} T_a^{'}}{1 + Y_{11} Z_a^{'}} f_c \ . \tag{13}$$

When the outer velocity feedback loop, described by

$$f_c = -Z_D v_b \ , \tag{14}$$

is implemented, the choice of the outer gain Z_D becomes important in order to guarantee a good performance. Fig. 6(left) shows the ratio of the frequency averaged power between power of the "passive" controller (without outer loop) and the active control (with outer loop) as a function of the outer velocity feedback gain, Z_D, assuming that the feedback loop is stable. The minimum of the function at Z_D = 2080 indicates the value of the gain that provides the greatest attenuation in terms of power. In this case, the attenuation is about 11.2 dB. In terms of stability, when the device is installed and the outer velocity feedback control loop is implemented based on the measurement of v_b, the Nyquist plot of the second term of equation (13) provides the means to determine the stability of the closed loop system. The theoretical active controller becomes unstable when the outer velocity feedback gain is greater than 2410. In the simulations, a velocity feedback gain of Z_D = 150 was chosen in order to guarantee a 6 dB stability margin when the additional phase shifts present in the experimental system are accounted for[12]. This implies, from Fig. 6(left), that an

attenuation of only about 4 dB can be achieved. When the outer velocity feedback loop in equation (14) is implemented, the base velocity becomes

$$v_b = \frac{Y_{10}}{1 + Y_{11} Z_a^{'} + Y_{11} T_a^{'} Z_D} f_p \ . \tag{15}$$

Substituting equation (15) into equation (10), the transmitted force, f_t, as a function of the bas velocity, v_b, is given by

$$f_t = -\frac{\left(j\omega m_a k_a - \omega^2 m_a c_a \right) \cdot \left(g_P + \frac{g_I}{j\omega} + j\omega (g_V + Z_a) \right) - j\omega^3 Z_a Z_D}{\left(-\omega^2 m_a + j\omega c_a + k_a + g_P + \frac{g_I}{j\omega} + j\omega g_V \right) j\omega Z_a} v_b \ . \tag{16}$$

Once the base velocity in equation (15) is computed, then the transmitted force in equation (16) can be obtained and therefore the total power can be calculated. This is plotted in Fig. 6(right). Although the difference with the optimal solution is still large, useful reductions in power are predicted, which shows that the modified inertial actuator can be used effectively in reducing the vibration of panels. The impedance presented by the active mount to the system is given by equation (16). The impedance is not passive, unlike the previous case, and it is mainly damping dominated at frequencies greater than the inertial actuator's resonance frequency. This is due to the choice of the local feedback gains, and in particular the derivative term within the PID controller. In conclusion, the modified inertial actuator with outer velocity feedback loop is an effective way of adding damping to the system.

When the outer control gain Z_D is chosen to be the equivalent impedance described in equation (9), the control system turns out to be unstable. If the outer feedback controller is an integrator of the form $Z_D = \frac{k_D}{j\omega}$, interesting results are obtained. Choosing such a control impedance implies that only the first part of the optimal impedance in equation (9) is considered. In other words, k_D is chosen to be the low frequency passive approximation of the optimal solution. In particular, when k_D = 550,000 N/m, the closed loop system turns out to be conditionally stable, and a 6 dB stability margin is guaranteed. The total power for this case shows very good reductions of the total power due to the modified inertial actuator and the outer controller, based on the passive approximation of the optimal solution. Unfortunately in real systems, due to low frequency phase shifts of the electronic components[12], the stability margin of the system is greatly reduced and the performance of the closed loop system is not dissimilar to the outer velocity feedback case.

5 EXPERIMENTS ON ACTIVE VIBRATION SUPPRESSION WITH THE MODIFIED INERTIAL ACTUATOR

In this section we consider the practical use of an inertial actuator with local feedback for the active suppression of a vibrating flexible plate. The arrangement is illustrated in Fig. 7. It consists of a flexible steel plate 700mm × 500mm × 1.85mm, clamped on the two longer sides[13], on which is mounted a modified inertial actuator. The primary force is provided by an LDS Ling 401 shaker, placed underneath the plate.

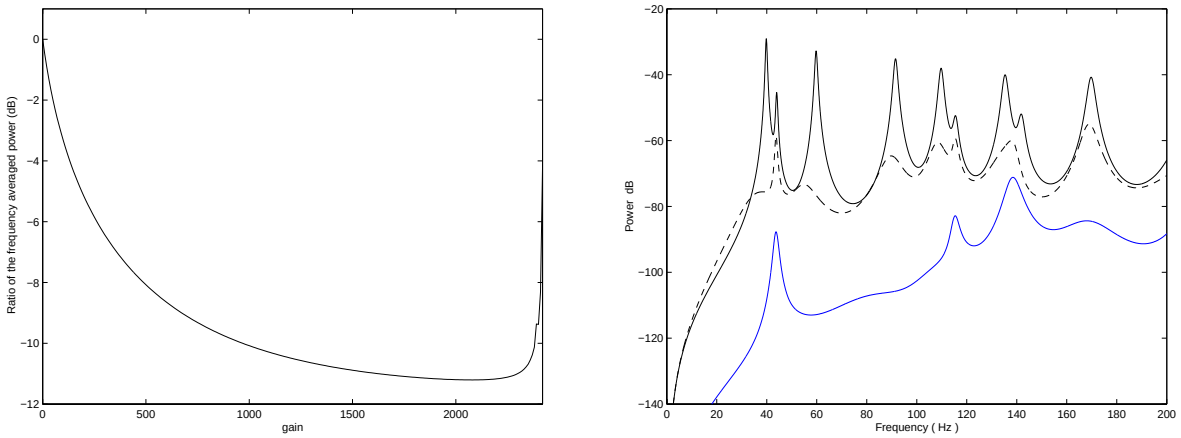

Figure 6. Left: ratio of the frequency averaged total power transmitted to the plate with the modified actuator before and after the outer feedback loop is implemented, as a function of the outer velocity feedback gain Z_D. The minimum of the function at Z_D = 2080 indicates the value of the gain that provides the greatest attenuation (about 11.2 dB) in terms of power. The active controller becomes unstable for outer velocity gains Z_D > 2410. The distance between primary and secondary forces is 2 cm. Right: total power transmitted to the finite plate due to the primary force only (solid), the primary and secondary forces when the optimal feedforward solution is applied (faint), and when the feedback system, based on the modified inertial actuator and an outer feedback loop with Z_D = 150, is applied (dashed). The distance between primary and secondary force is 2 cm.

The inertial actuator used for the experiments to produce the control force was a mechanically modified version of an Active Tuned Vibration Absorber (ATVA) manufactured by ULTRA Electronics, from which the internal springs were removed, leaving the proof-mass (m_a = 0.24 Kg) attached to the case by eight thin flexible supports. This modification in the stiffness (so that k_a = 2000 N/m) changed the actuator resonance frequency from 73.8 Hz to 14.5 Hz [19]. The measured damping ratio was used to estimate the damping factor as c_a = 18 N/ms^{-1}. An inner displacement feedback loop is used to modify the response of the inertial actuator, as discussed above, and an outer velocity feedback system is used to provide active skyhook damping for the equipment. In this experimental configuration, an outer velocity feedback control gain $Z_D = 150$ was chosen, which guarantees a 6 dB stability margin. The control performance of the active vibration suppression system with the modified inertial actuator has been examined based on the kinetic energy. To calculate the true kinetic energy of the system, the vibration of both the rigid body modes and the flexible body modes would have to be accounted for. In the experiments, however, only the plate velocities at 40 locations were measured, when the modified inertial actuator with outer velocity feedback loop was installed at the same location as described above. The sum of squared velocities at each location is therefore used to evaluate the control performance of the system. Fig. 8 shows the predicted and experimental results, which lead to similar conclusions as those drawn in the previous section. Theory and measurements agree well, showing up to 20 dB reduction in the vibration level and demonstrating the effectiveness of the modified inertial actuator.

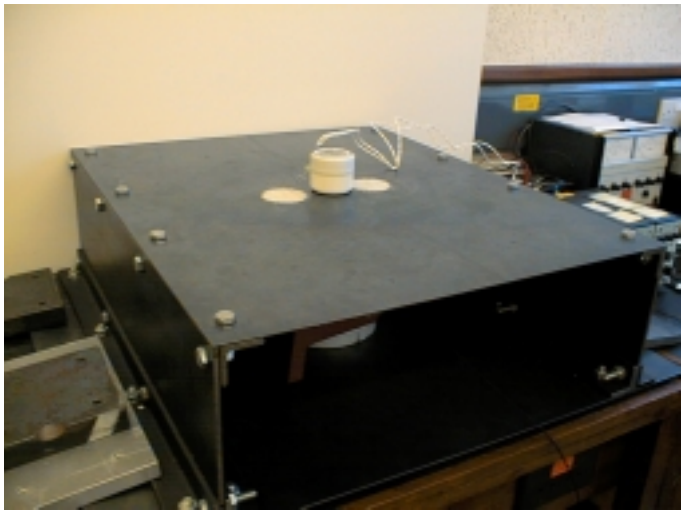

Figure 7. The experimental arrangement, which consists of a finite flexible plate, driven by a primary force (shaker underneath), and controlled by a modified ULTRA Electronics inertial actuator placed on the flexible plate.

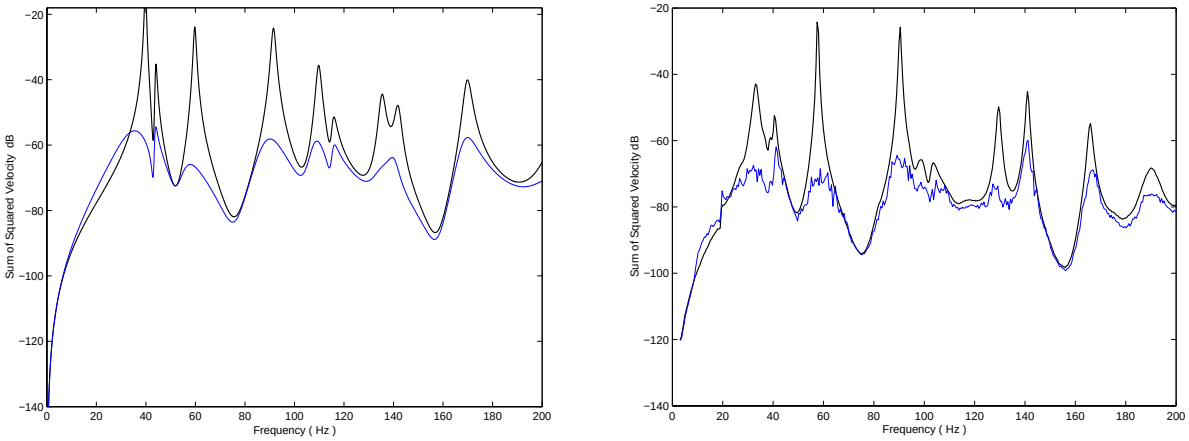

Figure 8. Predicted (left) and measured (right) sum of square velocities of the plate when no control is implemented (solid), and when both the modified inertial actuator and the outer velocity feedback loop are implemented with Z_D = 150 (faint).

6 VARIATION OF PERFORMANCE WITH THE LOCATION OF THE MODIFIED INERTIAL ACTUATOR

The objective of this section is to compare the previous results with solutions obtained by placing the modified inertial actuator with outer velocity feedback loop in other locations on the flexible plate. The primary force is assumed to be at a location P_0 = (0.32 m, 0.27 m) which guarantees that a sufficient number of modes are excited, while the controller, based on the modified inertial actuator, is assumed to be installed in turn on the plate at different locations. For this purpose, 500 potential secondary locations were selected. When the outer velocity feedback loop is implemented, the choice of the outer gain Z_D becomes important in order to guarantee a certain stability margin and good performance. As Fig. 6(left) shows, the ratio of the frequency averaged power between power of the “passive” controller (without outer loop) and the active control (with outer loop), as a function of the outer velocity feedback gain is Z_D, has a minimum, which indicates the value of the gain that provides the greatest attenuation in terms of power. When the active control, based on the

modified inertial actuator with outer velocity feedback loop, is implemented, the value of the feedback control gain Z_D that minimises the ratio of the frequency averaged power can be computed at each of the 500 selected locations on the plate, and is shown in Fig. 9(left). For each case, the stability of the closed loop system was guaranteed, although no specific stability margin was set. Depending on the location, the maximum gain Z_D before instability can change considerably, but the gain which minimises the ratio of the frequency averaged power was always computed to be less or equal than the stability limit. In Fig. 9(left) three main regions can be identified: around the location of the primary force high outer loop gains are needed in order to achieve the best attenuation possible with the active controller. High gains are also required close to the clamped edges. In the rest of the plate, although there are some differences, lower gains are needed. Fig. 9(right) shows the contour plot of the ratio of the frequency averaged power when the gains in Fig. 9(left) are used in the outer feedback loop controller. In other words, Fig. 9(right) shows the best attenuation that can be obtained with the active controller for that specific primary force location. If the active controller is placed near the primary force, average attenuations of up to 12.9 dB can be achieved within the selected frequency range between 0 Hz and 200 Hz, using the high outer gains shown in Fig. 9(left). This attenuation is decreased down to about 9 dB if the active controller is installed about 8 cm away from the primary force, where the *x* direction seems to be a little more privileged than the *y* direction in terms of attenuation. Although high gains are needed along the edges the attenuation is not significant, while in the rest of the plate attenuations, which vary from 2.3 dB to 5.4 dB, can be obtained, depending on the location of the secondary force.
In summary, the performance of the control strategy, based on the modified inertial actuator with outer velocity feedback control, depends on both the relative distance between primary and secondary forces as well as their absolute location on the plate. Ideally, the best solution would be to install the controller as close as possible to the primary disturbance.

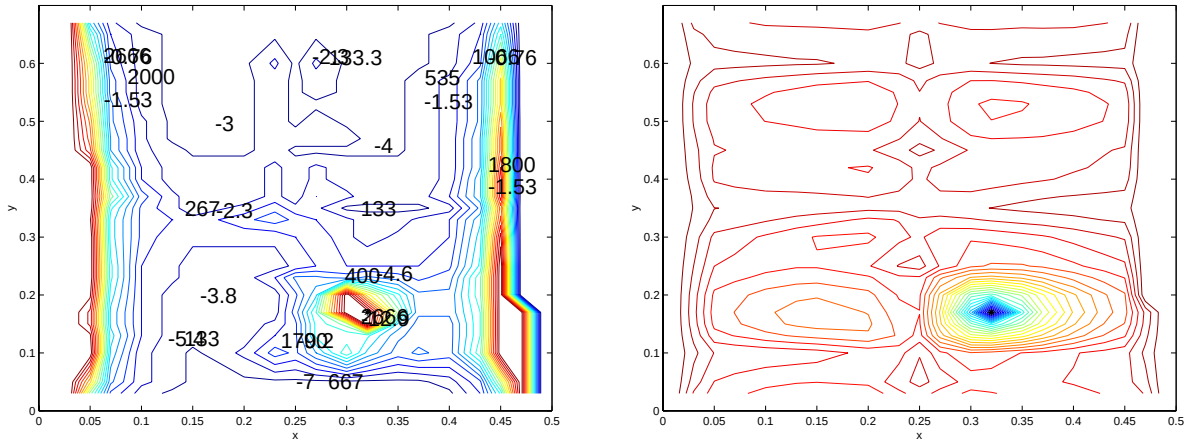

Figure 9. Left: contour plot of the outer velocity feedback gain Z_D which, for a specific location, provides the minimum of the ratio of the frequency averaged power between power of the plate with no actuator and the plate with the modified inertial actuator and outer velocity feedback loop, as a function of the *x* and *y* position of the controller on the flexible plate. The location of the primary force is indicated with a *. Right: contour plot of the ratio of the frequency averaged power between power of the plate with no actuator and the plate with the modified inertial actuator and outer velocity feedback loop, as a function of the *x* and *y* position of the controller on the flexible plate. The controller is based on the modified inertial actuator with outer velocity feedback loop.

7 CONCLUSIONS

In this study the total power of the forces exerting on a structure was minimised and a comparison was made between optimal solutions and the performance of various passive and active control treatments involving inertial actuators. In particular, the optimised impedance for global control was compared to the performance of a modified inertial actuator. It was found that, although the optimal

impedance is able to provide a more substantial total power reduction than the other treatments, the modified inertial actuator can still guarantee a good power reduction, especially when combined with an outer velocity feedback controller. This seems to be a very promising solution to the vibration suppression problem, even though attention must be paid to the location of the secondary force in order to achieve the best possible attenuation.
In using an inertial actuator for active vibration isolation, the resonance frequency should be lower than the first natural frequency of the system under control and it should be well damped. Actuators with very low resonance frequencies, however, have large static displacements due to gravity. The modified inertial actuator solves this problem. It is based on an inertial actuator and a local PID feedback loop which uses the measurement of the relative displacement between the actuator base and the actuator moving mass. The control law is the sum of an integral term, which provides self-levelling and solves the sagging problem, a derivative term, which provides the device with sufficient initial damping to guarantee a very good stability margin, and a positive or negative proportional term, which determines the actuator resonance frequency.

8 REFERENCES

1. M.J.Brennan and J. Dayou 2000, *Journal of Sound and Vibration*, 232, No. 3, 585-600. Global Control of Vibration using a Tunable Vibration Neutralizer.
2. O.Bardou, P. Gardonio, S.J.Elliott and R.J.Pinnington 1997, *Journal of Sound and Vibration*, 208, No. 1, 111-151. Active Power Minimization and Power Absorption in a Plate with Force and Moment Excitation.
3. S.J.Elliott, P.Joseph, P.A.Nelson and M.E.Johnson 1991, *Journal of Acoustic Society of America*, 90, No. 5, 2501-2512. Power Output Minimizations and Power Absorption in the Active Control of Sound.
4. D.W.Miller, S.R.Hall and A.H.von Flotow 1990, *Journal of Sound and Vibration*, 140, No. 3, 475-497. Optimal Control of Power Flow at Structural Junctions.
5. S.J.Elliott, M. Serrand and P. Gardonio 2001, *ASME Journal of Vibration and Acoustics*, 123, 250-261. Feedback stability limits for active isolation systems with reactive and inertial actuators.
6. R.E.D.Bishop and D.C.Johnson 1960, *The Mechanics of Vibration*, Cambridge University Press.
7. A.W.Leissa 1969, *NASA SP-160*, Vibration of Plates.
8. C.R.Fuller, S.J.Elliott and P.A.Nelson 1997, *Active Control of Vibration*, Academic Press.
9. L.Benassi and S.J.Elliott 2003 *Journal of Sound and Vibration*. Active Vibration Isolation using an Inertial Actuator with Local Displacement Feedback Control. *To be published.*
10. L.Benassi and S.J.Elliott 2003 *Journal of Sound and Vibration.* The Equivalent Impedance of Power-Minimising Vibration Controllers on Plates. *To be published.*
11. L.Benassi and S.J.Elliott 2004 *Journal of Sound and Vibration*. Global Control of a Vibrating Plate using a Feedback-Controlled Inertial Actuator. *Submitted.*
12. M.J.Brennan, K.A.Ananthganeshan and S.J.Elliott 2002 *Proc. ACTIVE2002* and submitted to *ASME Journal of Vibration and Acoustics*. Low and high frequency instabilities in feedback control of vibrating single-degree-of-freedom systems.
13. L.Benassi, S.J.Elliott and P.Gardonio 2003 *Journal of Sound and Vibration*. Active Vibration Isolation using an Inertial Actuator with Local Force Feedback Control. *To be published.*